

RADIUS OF CURVATURE OF
LAGUERRE-GAUSSIAN BEAM

S. ÇAY

SAİM ÇAY

SEPTEMBER, 2012

ÇANKAYA UNIVERSITY

ÇANKAYA UNIVERSITY
GRADUATE SCHOOL OF NATURAL AND APPLIED SCIENCES
ELECTRONIC AND COMMUNICATION ENGINEERING

MASTER THESIS

RADIUS OF CURVATURE OF LAGUERRE-GAUSSIAN BEAM

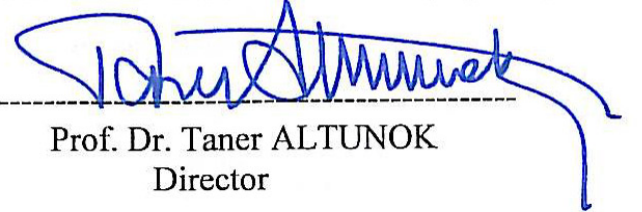
SAİM ÇAY

SEPTEMBER, 2012

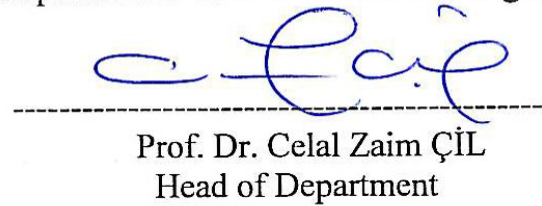
Title of Thesis : **Radius of Curvature of Laguerre-Gaussian Beam**

Submitted by : Saim ÇAY

Approval of the Graduate School of Natural and Applied Sciences, Çankaya University


Prof. Dr. Taner ALTUNOK
Director

I certify that this thesis satisfies all the requirements as a thesis for the degree of Master of Science.





Prof. Dr. Celal Zaim ÇİL
Head of Department

This is to certify that we have read this thesis and that in our opinion it is fully adequate, in scope and quality, as a thesis for the degree of Master of Science.


Prof. Dr. Yusuf Ziya UMUL
Supervisor

Examination Date: 11.09.2012

Examining Committee Members:

Assist. Prof. Dr. Barbaros PREVEZE (Çankaya University) 
Prof. Dr. Yusuf Ziya UMUL (Çankaya University) 
Research Assist. Filiz SARI (Ankara University) 

STATEMENT OF NON PLAGIARISM

I hereby declare that all information in this document has been obtained and presented in accordance with academic rules and ethical conduct. I also declare that, as required by these rules and conduct, I have fully cited and referenced all material and results that are not original to this work.

Name, Last Name : SAİM ÇAY

Signature : *Saim*

Date : 13.06.2013

ABSTRACT

RADIUS OF CURVATURE OF LAGUERRE-GAUSSIAN BEAM

ÇAY, Saim

M.Sc., Department of Electronic and Communication Engineering

Supervisor: Prof. Dr. Yusuf Z. UMUL

September 2012, 26 pages

In this thesis, the radius of curvature of Laguerre-Gaussian beam is formulated for turbulent atmosphere and analyzed numerically for various radial and angular mode numbers, the source size, propagation distance and wavelength in moderate, high and no turbulence levels. Results have shown that Laguerre-Gaussian beam approximates to Gaussian beam and radius of curvature of Laguerre-Gaussian beam reduces with increasing turbulence levels. The results have also shown that the radius of curvature of Laguerre-Gaussian beam increases with increasing source sizes and changes slowly with longer wavelengths.

Keywords: Gaussian beam, radius of curvature, Laguerre-Gaussian beam, Gaussian beam intensity, Gaussian beam width

ÖZET

LAGUERRE-GAUSSIAN IŞIK DEMETİ EĞRİLİK YARIÇAPI

ÇAY, Saim

Yüksek Lisans, Elektronik ve Haberleşme Mühendisliği Bölümü

Tez Yöneticisi: Prof. Dr. Yusuf Z. UMUL

Eylül 2012, 26 sayfa

Tezde, Laguerre-Gaussian ışık demetinin eğrilik yarıçapı türbülanslı atmosfer için formüle edilmiş, ve çeşitli radyal ve açısız mod numaraları, kaynak boyutu, yayılım uzaklığı için yüksek ve orta türbülans seviyeleri ile türbülansın olmadığı durumlarda nümerik olarak incelenmiştir. Sonuçlar, Laguerre-Gaussian ışık demetinin, Gaussian ışık demetine yakınsadığını ve artan türbülans seviyeleriyle Laguerre-Gaussian ışık demetinin eğrilik yarıçapının azaldığını göstermiştir. Ayrıca, sonuçlar Laguerre-Gaussian ışık demetinin eğrilik yarıçapının kaynak boyutunun büyümesiyle arttığını ve artan dalga boyuyla yavaşça değiştiğini de göstermiştir.

Anahtar Kelimeler: Gaussian ışık demeti, eğrilik yarıçapı, Laguerre-Gaussian ışık demeti, Gaussian ışık şiddeti, Gaussian ışık demeti genişliği

ACKNOWLEDGMENT

During study of this thesis, I wish to present my deepest regards to my supervisor Prof. Dr. Yusuf Z. UMUL for his valuable assistance and contribution.

TABLE OF CONTENTS

STATEMENT OF NON PLAGIARISM.....	iii
ABSTRACT.....	iv
ÖZET	v
ACKNOWLEDGMENTS	vi
TABLE OF CONTENTS.....	vii
LIST OF TABLES	viii
LIST OF FIGURES	ix
LIST OF SYMBOLS AND ABBREVIATIONS	x
INTRODUCTION	1
CHAPTERS:	
1. LAGUERRE-GAUSSIAN BEAM	3
1.1. LAGUERRE FUNCTIONS.....	3
1.2. ASSOCIATED LAGUERRE FUNCTIONS.....	4
1.3. GAUSSIAN BEAM.....	5
1.4. OPTICAL PROPERTIES OF THE GAUSSIAN BEAM.....	5
1.4.1. Beam Width and Beam Divergence.....	6
1.4.2. Intensity and Power.....	7
1.4.3. Phase	8
1.4.4. Radius of Curvature	9
1.5. LAGUERRE-GAUSSIAN BEAM	10
2. RADIUS OF CURVATURE OF LAGUERRE-GAUSSIAN BEAM.....	11
2.1. DEVELOPMENT OF THE FORMULATION	11
2.2. NUMERICAL ANALYSIS OF THE FORMULATION	15
CONCLUSION.....	22
REFERENCES.....	24
CURRICULUM VITAE	26

LIST OF TABLES

Table 2.1. Radii of Curvatures and Rayleigh Ranges of Laguerre-Gaussian Beam for Different Radial and Angular Mode Numbers, under Conditions of Different Turbulence Levels	19
-----------------------------------------------------------------------------------------------------------------------------------------------------------------------------------	----

LIST OF FIGURES

Figure 1.1	The First Six Laguerre Polynomials Are Plotted in Matlab by Using Equation (1.2) to Show Behavior of These Laguerre Polynomials vs. x Values	4
Figure 1.2	The First Four Associated Laguerre Polynomials Are Plotted in Matlab by Using Equation (1.10) .This Figure Shows Associated Laguerre Polynomials vs. x Values at $m = 1$	5
Figure 1.3	Beam Width against Propagation Distance for a Gaussian Beam at Fixed Wavelength and Source Size.....	6
Figure 1.4	Normalized Intensity vs. Propagation Distance z for a Gaussian Beam at Fixed Wavelength, Source Size and $r = 0$	7
Figure 1.5	Radii of Curvatures of Two Circles. R_1 and R_2 Are Radii of These Circles ($R_1 > R_2$)	9
Figure 1.6	Radius of Curvature vs. Propagation Distance z in Free Space at Fixed Wavelength and Source Size.....	10
Figure 2.1	Radii of Curvatures vs. Propagation Distance z at Fixed Source Size, Wavelength and Moderate Turbulence Level	16
Figure 2.2	Radii of Curvatures vs. Propagation Distance z under Condition of Free Space at Fixed Wavelength and Source Size	17
Figure 2.3	Radii of Curvatures vs. Propagation Distance z at Fixed Wavelength, Source Size and High Turbulence Level.....	18
Figure 2.4	Radii of Curvatures vs. Source Size at Fixed Wavelength, Propagation Distance z and Moderate Turbulence Level	20
Figure 2.5	Radii of Curvatures vs. Source Size at Fixed Wavelength, Propagation Distance z and High Turbulence Level.....	20
Figure 2.6	Radii of Curvatures vs. Wavelength at Fixed Source Size, Propagation Distance z , and Moderate Turbulence Level	21

LIST OF SYMBOLS AND ABBREVIATIONS

α	:	Parameter Which Is Related to the Gaussian Source Size
α_s	:	Source Size
θ_z	:	Beam Divergence
κ	:	Spatial Frequency
λ	:	Wavelength
$\Psi(\kappa)$:	Spectrum Function
$\varphi(r, z)$:	Phase
$\omega(z)$:	Beam Width
A_c	:	Complex Amplitude
$b_r(z)$:	Radial Second Moment
$b_{r\theta}(z)$:	Radial-Angular Second Moment
$b_\theta(z)$:	Angular Second Moment
C_n^2	:	Structure Constant
FSO	:	Free Space Optic
$I(r, z)$:	Optical Intensity
I_0	:	Optical Intensity at Source
j	:	Imaginary Number
k	:	Wave Number
L_0	:	Outer Scale of Turbulence
l_0	:	Inner Scale of Turbulence
L_n^m	:	Associated Laguerre Polynomial with n and m
m	:	Angular Mode Number
n	:	Radial Mode Number
$R(z)$:	Radius of Curvature
T	:	Contribution of Turbulence

$U(r, z)$:	Complex Field Amplitude
$u_s(s, \phi_s, z)$:	Complex Field Amplitude of Laguerre-Gaussian Beam at Source ($z = 0$)
$u_r(r, \phi_r, z)$:	Complex Field Amplitude of Laguerre-Gaussian Beam at Receiver
*	:	Complex Conjugate

INTRODUCTION

Since A.G. Bell made free space optical communication using sunlight as an optical carrier [1], free space optics (FSO) has been an important study subject. Nowadays, FSO systems have become small size and lightweight. And they use very narrow beam as an optical carrier which provides a more secure channel. Also, in these systems, larger bandwidths can be obtained by increasing the carrier frequency [2]. Furthermore, these systems do not require any license for using of spectrum [3]. FSO systems are separated from other conventional communication systems by these advantages. Despite these advantages, FSO systems have also some disadvantages. Since FSO systems transmit highly directed beam, alignment and pointing become more difficult. Also this beam can be affected by atmospheric factors such as turbulence, rain, snow and fog [2].

In FSO systems, laser beams are mostly used to transmit data. Lasers consist of optical resonator, pumping system and laser medium (atoms) and produce coherent, monochromatic and highly directed beam. Because of the need of sending data farther with less attenuated signal, characteristics of the laser beam have become more important.

One of these laser beam characteristics is the beam profile and many of laser beams have the Gaussian-profile. Hence, optical properties of these laser beams, such as radius of curvature and scintillation, are studied for understanding how they are affected by atmospheric turbulence. Some of these studies are about radius of curvature of hyperbolic, sinusoidal, annular, dark hollow, flat topped Gaussian beams [4, 5] and scintillation of the Laguerre-Gaussian beam and the lowest order Bessel-Gaussian beam [6, 7].

The objectives of this study are to obtain a formulation for the radius of curvature of the Laguerre-Gaussian beam, examine effects of various turbulence levels on the radius of curvature of the Laguerre-Gaussian beam numerically, show

that the Laguerre-Gaussian beam propagation profile acts as Gaussian propagation profile and compare the Gaussian beam with the Laguerre-Gaussian beam.

In Chapter I, Laguerre and associated Laguerre functions, Gaussian beam and its optical properties, which are complex field amplitude, intensity, power, beam width, beam divergence, depth of focus, phase and the radius of curvature, are mentioned briefly. So, fundamental information is given about behavior of the Laguerre-Gaussian beam.

In the first part of Chapter II, the radius of curvature of the Laguerre-Gaussian beam is developed analytically in turbulent atmosphere. In the second part of Chapter II, the radius of curvature of the Laguerre-Gaussian beam is analyzed numerically with the help of Matlab under certain conditions. The obtained figures are commented. And these figures show that the Laguerre-Gaussian beam follows trend of the Gaussian beam.

In Conclusion, this thesis is summarized briefly. Also, behavior of the Laguerre-Gaussian beam is commented on the results. Some useful data is provided for the application and the design of free space optical communication systems.

CHAPTER I

LAGUERRE-GAUSSIAN BEAM

1.1. LAGUERRE FUNCTIONS

Laguerre equation arises in solution of the radial portion of the Schrödinger equation for one-electron atom as Hydrogen. Laguerre functions and polynomials are important for studying of behavior of some physical systems in quantum mechanics [8]. Laguerre function is a solution of Laguerre differential equation which is expressed by

$$xy'' + (1 - x)y' + ny = 0. \quad (1.1)$$

n is a real number. It has singularities at $x = 0$ and $x = \infty$. For $x = 0$, it may be found one solution in the form of Frobenius series. This solution is given in [8] as

$$L_n(x) = \sum_{k=0}^n (-1)^k \frac{n!}{(k!)^2(n-k)!} x^k. \quad (1.2)$$

For this case, n is a non-negative integer. This solution is a polynomial which has order n . So, $L_n(x)$ is n th Laguerre polynomial. If equation (1.2) is calculated for the first six Laguerre polynomials, these polynomials will become,

$$L_0(x) = 1 \quad (1.3)$$

$$L_1(x) = -x + 1 \quad (1.4)$$

$$L_2(x) = \frac{x^2 - 4x + 2}{2!} \quad (1.5)$$

$$L_3(x) = \frac{-x^3 + 9x^2 - 18x + 6}{3!} \quad (1.6)$$

$$L_4(x) = \frac{x^4 - 16x^3 + 72x^2 - 96x + 24}{4!} \quad (1.7)$$

$$L_5(x) = \frac{-x^5 + 25x^4 - 200x^3 + 600x^2 - 600x + 120}{5!} \quad (1.8)$$

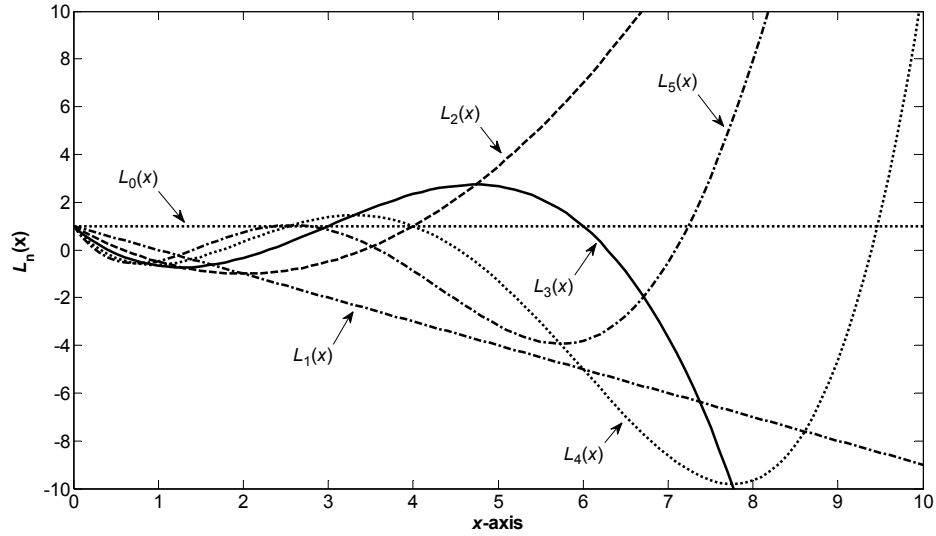


Figure 1.1 The first six Laguerre polynomials are plotted in Matlab by using equation (1.2) to show behavior of these Laguerre polynomials vs. x values

1.2. ASSOCIATED LAGUERRE FUNCTIONS

Associated Laguerre equation is given as

$$xy'' + (m + 1 - x)y' + ny = 0. \quad (1.9)$$

Equation (1.9) has singularities at $x = 0$ and $x = \infty$. Associated Laguerre function is any solution of this equation. If n and m are non-negative integers, solution of equation (1.9) is associated Laguerre polynomials which are given in [8] as

$$L_n^m(x) = \sum_{k=0}^n (-1)^k \frac{(n+m)!}{k!(n-k)!(k+m)!} x^k. \quad (1.10)$$

From equation (1.10), the first four associated Laguerre Polynomials will become,

$$L_0^m(x) = 1 \quad (1.11)$$

$$L_1^m(x) = -x + m + 1 \quad (1.12)$$

$$L_2^m(x) = \frac{x^2 - 2(m+2)x + (m+1)(m+2)}{2!} \quad (1.13)$$

$$L_3^m(x) = \frac{-x^3 + 3(m+3)x^2 - 3(m+2)(m+3)x}{3!} + \frac{(m+1)(m+2)(m+3)}{3!} \quad (1.14)$$

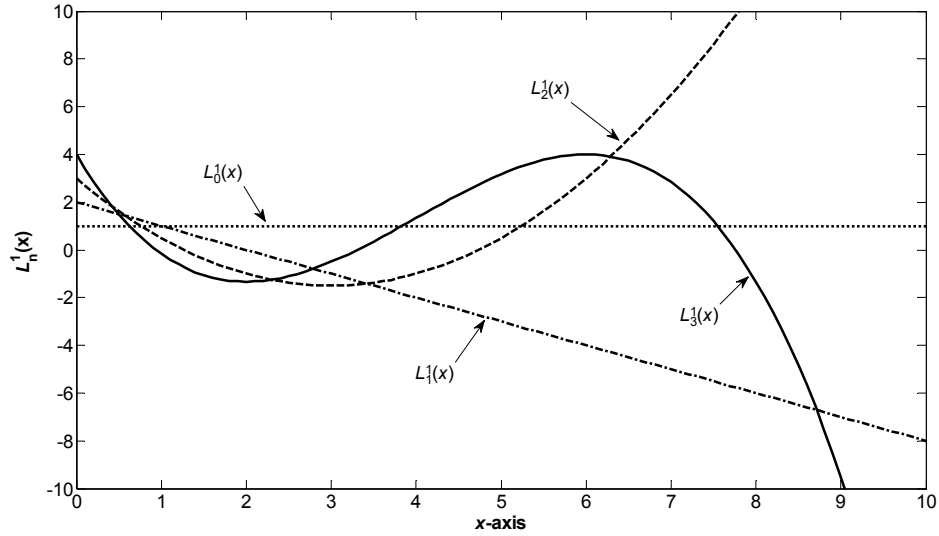


Figure 1.2 The first four associated Laguerre polynomials are plotted in Matlab by using equation (1.10). This figure shows associated Laguerre polynomials vs. x values at $m = 1$

1.3. GAUSSIAN BEAM

One of the most useful solutions of the paraxial Helmholtz equation is the Gaussian beam. Its intensity distribution is a Gaussian function in any transverse plane. Its complex field amplitude is given in [9] as

$$U(r, z) = A_0 \frac{\alpha_s}{\omega(z)} \exp\left(-\frac{r^2}{\omega^2(z)}\right) \exp\left[-j\left(kL - \tan^{-1}\frac{L}{z_R}\right) - j\frac{kr^2}{2R(z)}\right], \quad (1.15)$$

where r and z are respectively radial and propagation distances, λ is wavelength, $k = 2\pi/\lambda$ is the wavenumber, $\omega(z)$ is the beam width. And $R(z)$ is the radius of curvature. Rayleigh range is defined by $z_R = \pi\alpha_s^2/\lambda$. $\alpha_s = \sqrt{\lambda z_R/\pi}$ is source size and A_0 is the complex envelope.

1.4. OPTICAL PROPERTIES OF THE GAUSSIAN BEAM

Many lasers produce beams which are alike the Gaussian profile. That is, the beam is characterized by the Gaussian beam parameters. Hence, properties of the Gaussian beam are important. In the following sections, these properties of a Gaussian beam are briefly described.

1.4.1. Beam Width And Beam Divergence

For propagation of a Gaussian beam, beam width is known as spread of a beam from the z propagation axis. From [9], beam width is

$$\omega(z) = \alpha_s \sqrt{1 + \left(\frac{z}{z_R}\right)^2}, \quad (1.16)$$

where α_s is beam waist or source size, which is minimum of the beam width at $z = 0$. And $2\alpha_s$ is known as the spot size.

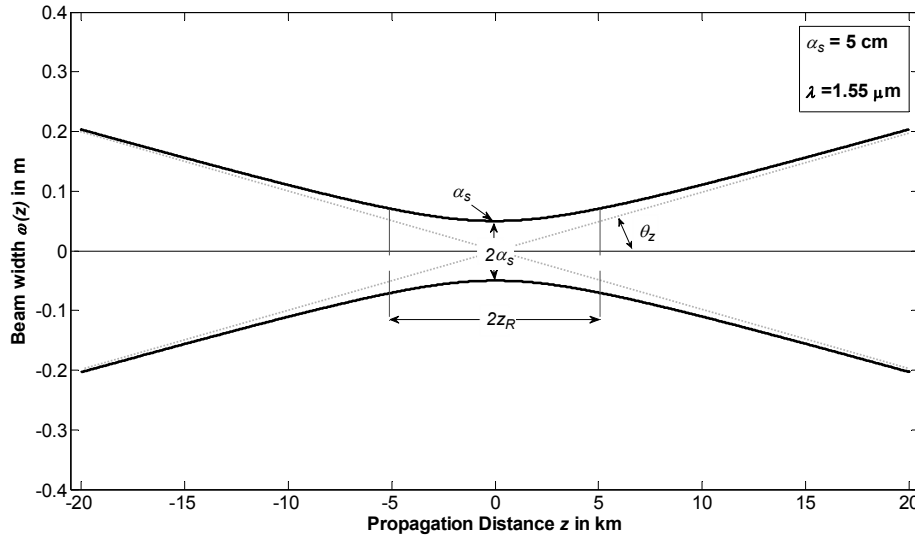


Figure 1.3 Beam width against propagation distance for a Gaussian beam at fixed wavelength and source size

Figure 1.3 is plotted by using equation (1.16) in Matlab. Also Figure 1.3 includes $-\omega(z)$ for the best view of all the terms. As shown in Figure 1.3, the beam expands for larger z value and so, the beam width increases.

θ_z is beam divergence, which is illustrated in Figure 1.3. If it is assumed that $z_R \ll z$, angle with z -axis of the Gaussian beam (θ_z) can be written by using the paraxial approach as

$$\tan(\theta_z) \approx \theta_z = \frac{\alpha_s}{z_R} = \frac{\lambda}{\pi\alpha_s}. \quad (1.17)$$

If the wavelength becomes shorter or the beam waist becomes larger, the beam divergence will become smaller. So, highly directional beam can be obtained.

Depth of focus is $2z_R$ long, where the Gaussian beam achieves the best focus. Center of this length is at the beam waist ($z = 0$). The depth of focus is illustrated in Figure 1.3 and expressed by

$$2z_R = \frac{2\pi\alpha_s^2}{\lambda}. \quad (1.18)$$

From equation (1.18), it is clear that the depth of focus is directly proportional with the area of spot size ($\pi\alpha_s^2$) [9] and inversely proportional with the wavelength.

1.4.2. Intensity And Power

Optical intensity can be defined as power per unit area ($watt/m^2$). Optical intensity of a Gaussian beam is given in [9] by,

$$I(r, z) = |U(r, z)|^2. \quad (1.19)$$

If equation (1.15) is substituted into equation (1.19), intensity of Gaussian beam will become

$$I(r, z) = I_0 \left[\frac{\alpha_s}{\omega(z)} \right]^2 \exp \left[-\frac{2r^2}{\omega^2(z)} \right], \quad (1.20)$$

where I_0 is the intensity at source. The intensity is a Gaussian function of radial distance at any z value [9].

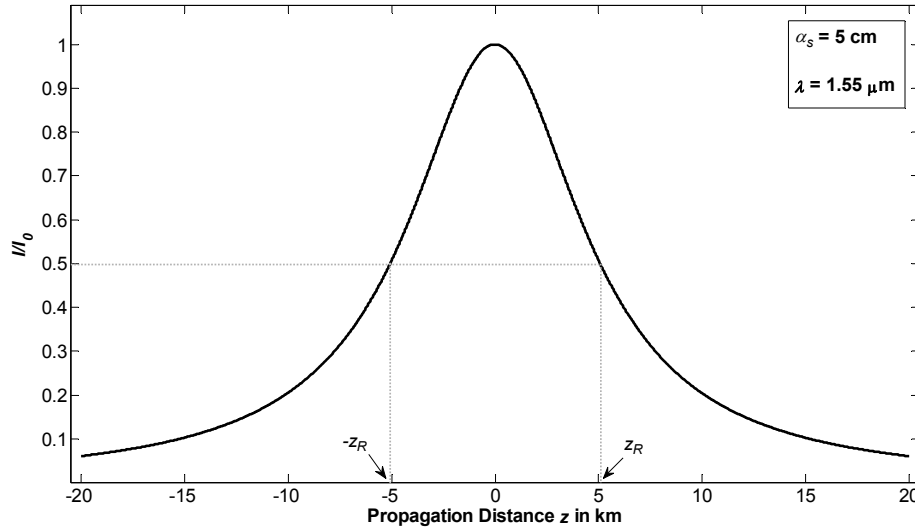


Figure 1.4 Normalized intensity vs. propagation distance z for a Gaussian beam at fixed wavelength, source size and $r = 0$

Figure 1.4 is plotted by using equation (1.6) at $r = 0$. In Figure 1.4, the intensity has its maximum value at $z = 0$ which is I_0 . And it reaches its half maximum value at $z = \pm z_R$. Finally, it decreases with increasing value of z .

Optical power of a Gaussian beam is integral of the optical intensity over any transverse plane and its unit is *watt*. It is expressed by

$$P(r, z) = \int_0^{\infty} I(r, z) 2\pi r dr. \quad (1.21)$$

So, if equation (1.20) is substituted into equation (1.21), total optical power will be

$$P_0 = \frac{1}{2} I_0 (\pi \alpha_s^2). \quad (1.22)$$

Equation (1.22) is independent of propagation distance z .

1.4.3. Phase

From equation (1.15), the phase of the Gaussian beam is

$$\varphi(r, z) = kz - \tan^{-1} \frac{z}{z_R} + \frac{kr^2}{2R(z)}. \quad (1.23)$$

At $r = 0$,

$$\varphi(r = 0, z) = kz - \tan^{-1} \frac{z}{z_R}. \quad (1.24)$$

The first term of equation (1.23) is the phase of plane wave and the latter term is phase retardation. The latter term also causes the delay of wavefront. Total phase delay from $z = -\infty$ to $z = +\infty$ is π . This phase delay is known as the Gouy effect [9].

1.4.4. Radius Of Curvature

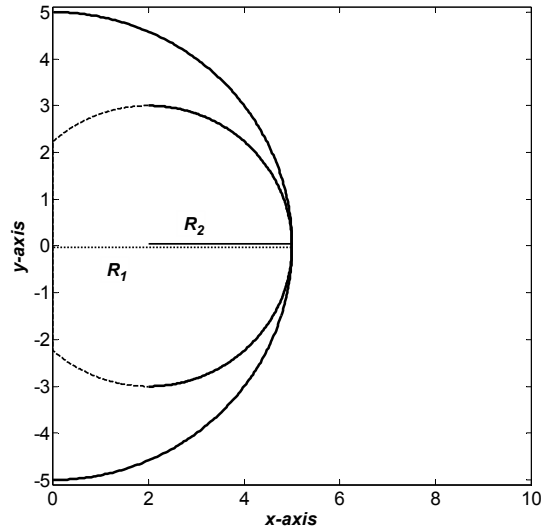


Figure 1.5 Radii of curvatures of two circles. R_1 and R_2 are radii of these circles ($R_1 > R_2$)

Radius of curvature is a number which determines curvature of any surface. In Figure 1.5, if radius of curvature becomes longer, the surface will become more flat. In the same way, the surface will become more curved for smaller radius of curvature. For a Gaussian beam, radius of curvature determines curvature of the wavefronts.

The third term of equation (1.23) is related to the curvature of wavefronts and the radius of curvature, $R(z)$, of a Gaussian beam is given in [9] as

$$R(z) = z \left[1 + \left(\frac{z_R}{z} \right)^2 \right]. \quad (1.25)$$

When Rayleigh range is substituted into equation (1.25), radius of curvature for a Gaussian beam can be expressed by

$$R(z) = 0.25z^{-1}(k^2\alpha_s^4 + 4z^2). \quad (1.26)$$

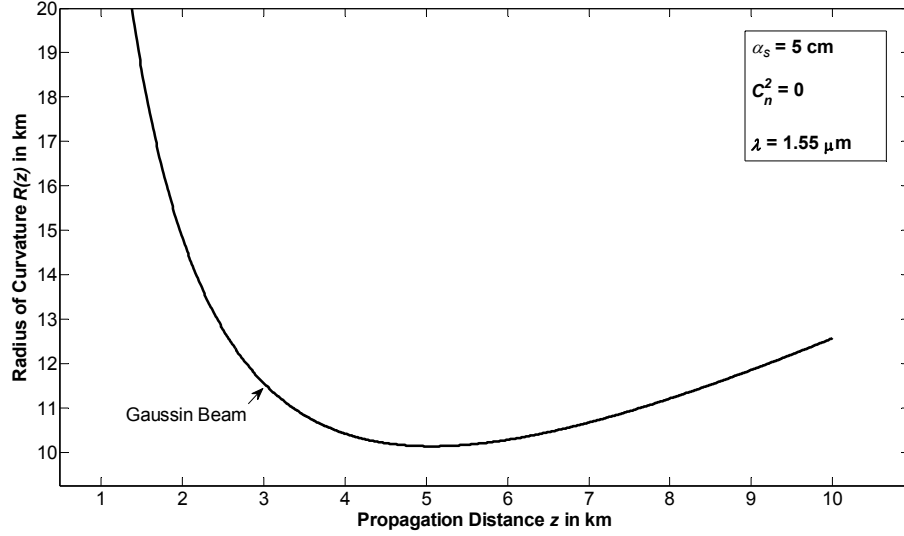


Figure 1.6 Radius of curvature vs. propagation distance z in free space at fixed wavelength and source size

Figure 1.6 is plotted by using equation (1.26) in Matlab. At $z = 0$, the radius of curvature is infinite. That is, at this point wavefronts are planar. And at $z = z_R$, it reaches its minimum value. After that point, radius of curvature increases with longer propagation distance.

1.5. LAGUERRE-GAUSSIAN BEAM

The Laguerre-Gaussian beam is another solution of the paraxial Helmholtz equation in cylindrical coordinates.

From equation (3) of [6], on receiver plane the complex field amplitude of Laguerre-Gaussian beam is

$$u_r(r, \phi_r, z) = A_c [-j\sqrt{2k\alpha r} \exp(j\phi_r)]^m \exp(jkz) \frac{(1 - 2j\alpha z)^n}{(1 + 2j\alpha z)^{m+n+1}} \times \exp\left(\frac{-k\alpha r^2}{1 + 2j\alpha z}\right) L_n^m\left(\frac{2k\alpha r^2}{1 + 4\alpha^2 z^2}\right), \quad (1.27)$$

where r and ϕ_r are radial coordinates, z is propagation distance, $k = 2\pi/\lambda$ is wavenumber, A_c is complex amplitude, $\alpha = 1/k\alpha_s^2$ is related to the Gaussian source size, n and m are respectively radial and angular mode numbers, j is $\sqrt{-1}$, and L_n^m is associated (generalized) Laguerre polynomial.

CHAPTER II

RADIUS OF CURVATURE OF LAGUERRE-GAUSSIAN BEAM

2.1. DEVELOPMENT OF THE FORMULATION

At a distance of z from the source plane on a receiver plane the radius of curvature is given in equation (1) of [4] as

$$R(z) = \frac{b_r(z) + \left(\frac{4}{3}\right)z^3T}{b_{r\theta}(z) + 2z^2T}, \quad (2.1)$$

where $b_r(z)$ is radial second moment and $b_{r\theta}(z)$ is radial-angular second moment. T represents contribution of turbulence, which is an integration over the entire range of spatial frequencies κ of the spectrum function $\Psi(\kappa)$. From equation (2) of [4], T is

$$T = \pi^2 \int_0^\infty \Psi(\kappa) \kappa^3 d\kappa. \quad (2.2)$$

For $\Psi(\kappa)$, modified von Kármán spectrum is applied in this thesis. From [2] $\Psi(\kappa)$ is,

$$\Psi(\kappa) = \frac{0,033C_n^2 \exp\left[-\left(\frac{l_0}{5,92}\right)^2 \kappa^2\right]}{\left[\kappa^2 + \left(\frac{2\pi}{L_0}\right)^2\right]^{11/6}}, \quad (2.3)$$

where C_n^2 is refractive-index structure constant, l_0 is inner scale and L_0 is outer scale. So, equation (2.2) can be written with equation (2.3) under the condition of $L_0 \rightarrow \infty$ as

$$T = 0.033\pi^2 C_n^2 \int_0^\infty \kappa^{-2/3} \exp\left[-\left(\frac{l_0}{5,92}\right)^2 \kappa^2\right] d\kappa. \quad (2.4)$$

Finally, by using equation (3.478.1) of [10] T becomes

$$T = 1,6393 \frac{C_n^2}{l_0^{1/3}}. \quad (2.5)$$

From (4) of [9], $b_r(z)$ and $b_{r\theta}(z)$ are

$$b_r(z) = b_r(0) + 2b_{r\theta}(0)z + b_\theta(0)z^2, \quad (2.6a)$$

$$b_{r\theta}(z) = b_{r\theta}(0) + b_\theta(0)z, \quad (2.6b)$$

where $b_r(0)$, $b_{r\theta}(0)$ and $b_\theta(0)$ are respectively radial, radial-angular and angular second moments at source. Terms of $b_{r\theta}(z)$, which are $b_{r\theta}(0)$ and $b_\theta(0)$, also exist in $b_r(z)$ as the coefficients of z and z^2 . Because of this, if $b_r(z)$ is obtained, the radius of curvature of the Laguerre-Gaussian beam is attained. From equation (7) of [4], b_r is

$$b_r(z) = \frac{\int_0^\infty \int_0^{2\pi} r^3 u_r(r, \theta) u_r^*(r, \theta) dr d\theta}{\int_0^\infty \int_0^{2\pi} s u_s(s, \phi) u_s^*(s, \phi) ds d\phi}. \quad (2.7)$$

Complex field amplitude on source plane from equation (1) of [6], its complex conjugate and complex conjugate of equation (1.27) are respectively expressed in the following manner:

$$u_s(s, \phi_s, z = 0) = A_c [-j\sqrt{2k\alpha s} \exp(-j\phi_s)]^m \exp(-k\alpha s^2) L_n^m(2k\alpha s^2), \quad (2.8a)$$

$$u_s^*(s, \phi_s, z = 0) = A_c^* [j\sqrt{2k\alpha s} \exp(j\phi_s)]^m \exp(-k\alpha s^2) L_n^m(2k\alpha s^2), \quad (2.8b)$$

$$u_r^*(r, \phi_r, z) = A_c^* [j\sqrt{2k\alpha r} \exp(-j\phi_r)]^m \exp(-jkz) \frac{(1 + 2j\alpha z)^n}{(1 - 2j\alpha z)^{m+n+1}} \times \exp\left(\frac{-k\alpha r^2}{1 - 2j\alpha z}\right) L_n^m\left(\frac{2k\alpha r^2}{1 + 4\alpha^2 z^2}\right), \quad (2.9)$$

where s and ϕ_s are radial coordinates at source, r and ϕ_r are radial coordinates at receiver, n and m are respectively radial and angular mode numbers, $\alpha = 1/k\alpha_s^2$ is related to the Gaussian source size, α_s is source size, $k = 2\pi/\lambda$ is wavenumber and j is $\sqrt{-1}$. From equation (2.7), numerator and denominator of $b_r(z)$ are respectively called I_r and I_s . I_r is

$$I_r = \int_0^{\infty} \int_0^{2\pi} r^3 u_r(r, \theta) u_r^*(r, \theta) dr d\theta. \quad (2.10a)$$

If equations (1.27) and (2.9) are substituted into equation (2.10a), I_r can be written as

$$I_r = \int_0^{\infty} \int_0^{2\pi} r^3 A_c A_c^* (2k\alpha)^m r^{2m} \frac{1}{(1 + 4\alpha^2 z^2)^{m+1}} \exp\left(\frac{-2k\alpha r^2}{1 + 4\alpha^2 z^2}\right) \times \left[L_n^m\left(\frac{2k\alpha r^2}{1 + 4\alpha^2 z^2}\right) \right]^2 dr d\theta. \quad (2.10b)$$

When integration of I_r with respect to θ is obtained, I_r will become

$$I_r = A_c A_c^* (2k\alpha)^m \frac{2\pi}{(1 + 4\alpha^2 z^2)^{m+1}} \int_0^{\infty} r^{2m+2} r \exp\left(\frac{-2k\alpha r^2}{1 + 4\alpha^2 z^2}\right) \times \left[L_n^m\left(\frac{2k\alpha r^2}{1 + 4\alpha^2 z^2}\right) \right]^2 dr. \quad (2.10c)$$

For the solution of equation (2.10c), equation (13) of [11] is used, which is

$$\int_0^{\infty} x^{t+1} \exp(-x) [L_n^t(x)]^2 dx = \frac{(2n + t + 1)(n + t)!}{n!}. \quad (2.11)$$

Parameters, which are used for adaptation of equation (2.10c) to equation (2.11), can be written as

$$t = m, \quad (2.12a)$$

$$x = \frac{2k\alpha r^2}{1 + 4\alpha^2 z^2}, \quad (2.12b)$$

and the derivative of equation (2.12b) is

$$dx = \frac{4k\alpha r}{1 + 4\alpha^2 z^2} dr. \quad (2.12c)$$

When equations (2.12a), (2.12b) and (2.12c) are substituted into equation (2.10c), I_r will become

$$I_r = A_c A_c^* (2k\alpha)^m \frac{2\pi}{(1 + 4\alpha^2 z^2)^{m+1}} \int_0^\infty x^{m+1} \exp(-x) [L_n^m(x)]^2 r \times \frac{(1 + 4\alpha^2 z^2)^{m+1} (1 + 4\alpha^2 z^2)}{(2k\alpha)^{m+1} 4k\alpha r} dx. \quad (2.13)$$

After some simplifications, finally I_r turns out to be

$$I_r = A_c A_c^* \frac{2\pi}{8k^2 \alpha^2} (1 + 4\alpha^2 z^2) \frac{(2n + m + 1)(n + m)!}{n!}. \quad (2.14)$$

I_s , which is denominator of $b_r(z)$, is

$$I_s = \int_0^\infty \int_0^{2\pi} s u_s(s, \phi) u_s^*(s, \phi) ds d\phi. \quad (2.15a)$$

If equations (2.8a) and (2.8b) are substituted into equation (2.15a), I_s is

$$I_s = \int_0^\infty \int_0^{2\pi} A_c A_c^* s^{2m} (2k\alpha)^m \exp(-2k\alpha s^2) [L_n^m(2k\alpha s^2)]^2 ds d\phi_s. \quad (2.15b)$$

In the same way, when integration of I_s with respect to θ is obtained, I_s will become

$$I_s = A_c A_c^* (2k\alpha)^m 2\pi \int_0^\infty s^{2m} \exp(-2k\alpha s^2) [L_n^m(2k\alpha s^2)]^2 s ds. \quad (2.15c)$$

Final equation of [12] is applied for the solution of equation (2.15c), which is

$$\int_0^\infty \exp(-x) (x)^m [L_n^m(x)]^2 dx = \frac{(n + m)!}{n!}. \quad (2.16)$$

For the adaptation of equation (2.15c) to (2.16), the following conversion is done:

$$x = 2k\alpha s^2, \quad (2.17a)$$

and the derivative of equation (2.17a) is

$$4k\alpha s ds = dx. \quad (2.17b)$$

If equations (2.17a) and (2.17b) are substituted into equation (2.15c), I_s will become

$$I_s = A_c A_c^* (2k\alpha)^m 2\pi \int_0^\infty \frac{x^m}{(2k\alpha)^m} \exp(-x) [L_n^m(2k\alpha s^2)]^2 s \frac{dx}{4k\alpha s}. \quad (2.18)$$

When simplifications are made, I_s turns out to be

$$I_s = A_c A_c^* \frac{2\pi(n+m)!}{4k\alpha n!}. \quad (2.19)$$

If equations (2.14) and (2.19), which are numerator and denominator of $b_r(z)$, are replaced into equation (2.7), $b_r(z)$ will be

$$b_r(z) = \frac{I_r}{I_s} = \frac{A_c A_c^* \frac{2\pi}{8k^2\alpha^2} (1 + 4\alpha^2 z^2) \frac{(2n+m+1)(n+m)!}{n!}}{A_c A_c^* \frac{2\pi(n+m)!}{4k\alpha n!}}. \quad (2.20)$$

$b_r(z)$ must be written as coefficients of z and z^2 to associate $b_r(z)$ with $b_{r\theta}(z)$. So, equation (2.21a) will turn to (2.21b) as follows:

$$b_r(z) = \frac{(1 + 4\alpha^2 z^2)(2n+m+1)}{2k\alpha}, \quad (2.21a)$$

$$b_r(z) = \frac{2n+m+1}{2k\alpha} + \frac{4\alpha^2(2n+m+1)}{2k\alpha} z^2. \quad (2.21b)$$

When the terms, which have same coefficients of $b_r(z)$ and $b_{r\theta}(z)$, are obtained from equation (2.21b), they are replaced in equation (2.6b). So, $b_{r\theta}(z)$ becomes

$$b_{r\theta}(z) = \frac{4\alpha^2(2n+m+1)}{2k\alpha} z. \quad (2.22)$$

Finally, when equations (2.21b) and (2.22) are substituted into equation (2.1), the radius of curvature of Laguerre-Gaussian beam is obtained as

$$R(z) = \frac{\frac{(1 + 4\alpha^2 z^2)(2n+m+1)}{2k\alpha} + \frac{4}{3} z^3 T}{\frac{4\alpha^2(2n+m+1)}{2k\alpha} z + 2z^2 T}. \quad (2.23)$$

2.2. NUMERICAL ANALYSIS OF THE FORMULATION

In this section, equation (2.23) is analyzed numerically by using Matlab. During this analysis, unless specified otherwise, source size and wavelength are respectively

taken as 5 cm and $1.55 \mu\text{m}$, since these values are used commonly in the optical systems. All the figures in this section are also scaled for the best view of each plot's trend. When radial and angular mode numbers are equal to zero, the radii of curvatures of the Laguerre-Gaussian and the Gaussian beams should be the same. Because of this, Laguerre-Gaussian beam is mentioned as Gaussian beam at $n = 0$ and $m = 0$ in the figures.

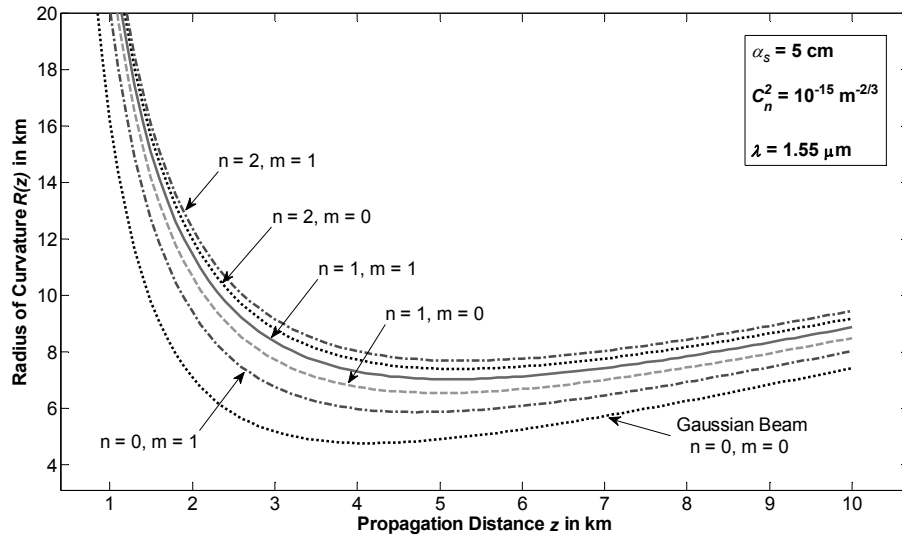


Figure 2.1 Radii of curvatures vs. propagation distance z at fixed source size, wavelength and moderate turbulence level

In Figure 2.1, for different radial and angular mode numbers, the radius of curvature of the Laguerre-Gaussian beam variations are plotted vs. propagation distance at fixed wavelength, source size and moderate turbulence level ($C_n^2 = 10^{-15} \text{ m}^{-2/3}$). Figure 2.1 shows that the radius of curvature of the Laguerre-Gaussian beam is infinite at first, and then the radius of curvature reaches finite value and decreases with increasing propagation distance. The radius of curvature reaches its minimum value and after that point increases with longer propagation distance. For higher radial and angular mode numbers, the radius of curvature will be higher. In the same way, for smaller radial and angular mode numbers, the radius of curvature will be lower.

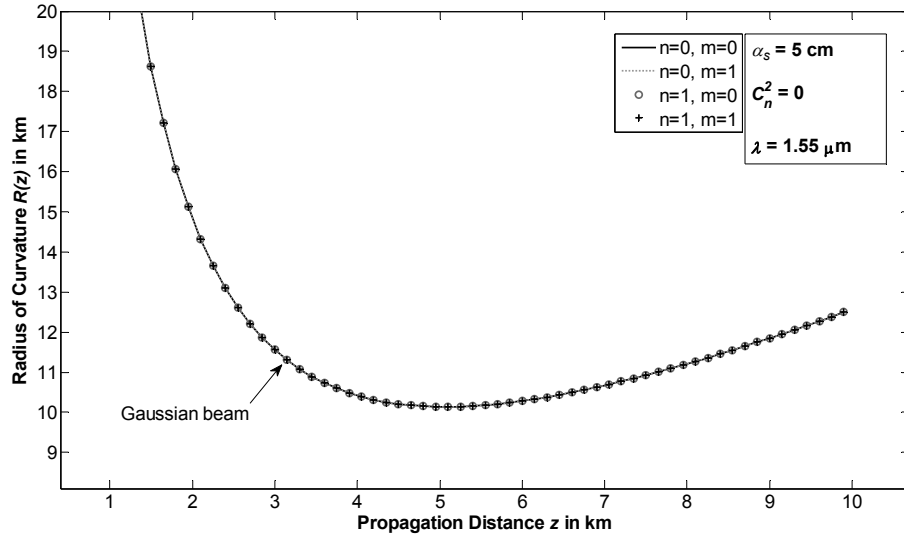


Figure 2.2 Radii of curvatures vs. propagation distance z under condition of free space at fixed wavelength and source size

In Figure 2.2, for different radial and angular mode numbers, the radius of curvature of the Laguerre-Gaussian beam variations are plotted vs. propagation distance at fixed wavelength, source size and under condition of free space (i.e. $C_n^2 = 0$). Figure 2.2 shows that under free space condition, the radius of curvature of the Laguerre-Gaussian beam acts as independent of radial and angular mode number. Clearly it is seen that equation (2.23) will become $R(z) = 0.25z^{-1}(k^2\alpha_s^4 + 4z^2)$ for $C_n^2 = 0$ which is equal to the radius of curvature of a pure Gaussian beam. As a result, without turbulence, behaviors of the radius of curvature of the Laguerre-Gaussian beam and the pure Gaussian beam are the same.

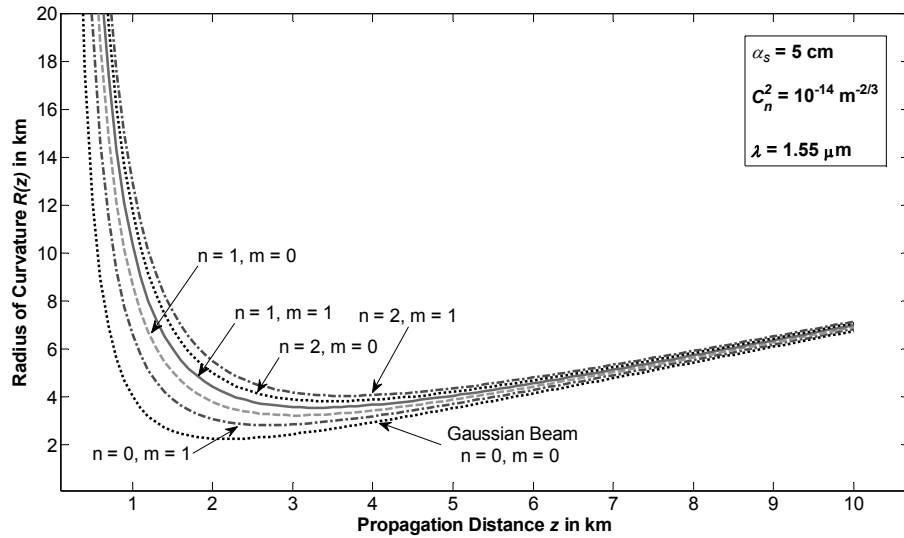


Figure 2.3 Radii of curvatures vs. propagation distance z at fixed wavelength, source size and high turbulence level

In Figure 2.3, for different radial and angular mode numbers, the radius of curvature of the Laguerre-Gaussian beam variations are plotted vs. propagation distance at fixed source size, wavelength and high turbulence level ($C_n^2 = 10^{-14} \text{ m}^{-2/3}$). Figure 2.3 shows that the radius of curvature decreases significantly with increasing turbulence levels for all radial and angular numbers and this increase in turbulence levels causes to decrease of the differences between radii of curvatures for all beams.

Obviously, from Figures 2.1, 2.2 and 2.3 it is seen that increasing turbulence levels decrease the radius of curvature. Also, it is clear that trend of the Laguerre-Gaussian beam is similar to a Gaussian beam.

C_n^2 in $m^{-2/3}$	n	m	$R(z)$ in km	z_R in km
10^{-15}	0	0	4.761	4.132
	0	1	5.855	4.725
	1	0	6.538	4.997
	1	1	7.023	5.141
	2	0	7.389	5.220
	2	1	7.678	5.265
0	0	0	10.134	5.067
	0	1		
	1	0		
	1	1		
10^{-14}	0	0	2.250	2.179
	0	1	2.831	2.691
	1	0	3.235	3.028
	1	1	3.554	3.282
	2	0	3.821	3.486
	2	1	4.052	3.655

Table 2.1 Radii of curvatures and Rayleigh ranges of Laguerre-Gaussian beam for different radial and angular mode numbers, under conditions of different turbulence levels

The radius of curvature of the Gaussian beam achieves its minimum value at $z = z_R$. Because of Laguerre-Gaussian beam also acts similarly to a Gaussian beam, the Rayleigh ranges of all beams can be obtained from Figures 2.1, 2.2 and 2.3. These values are shown in Table 2.1. Within one Rayleigh range, the Gaussian beam carries its 50% of normalized intensity, which is shown in Figure 2.4. Beyond that distance, the beam spreads more rapidly and loses its focus. From Table 2.1, the Laguerre-Gaussian beams have longer Rayleigh ranges. Also, their Rayleigh ranges decrease with strong turbulence.

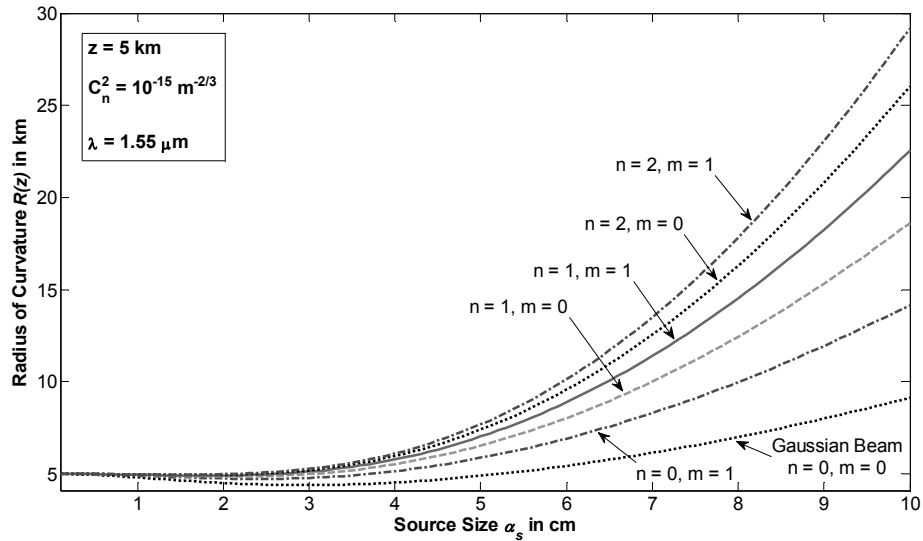


Figure 2.4 Radii of curvatures vs. source size at fixed wavelength, propagation distance z and moderate turbulence level

In Figure 2.4, for different radial and angular mode numbers, the radius of curvature of the Laguerre-Gaussian beam variations are plotted vs. source size at fixed wavelength, propagation distance z and moderate turbulence level ($C_n^2 = 10^{-15} \text{ m}^{-2/3}$). Figure 2.4 shows that at smaller source size, the radii of curvatures are around propagation distance and at bigger source size, the radii of curvatures increase sharply with increasing radial and angular mode numbers.

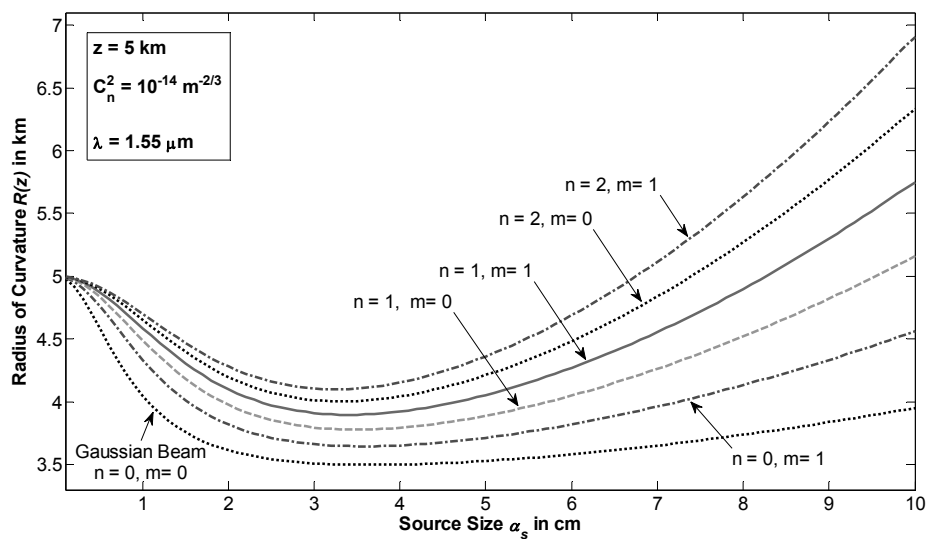


Figure 2.5 Radii of curvatures vs. source size at fixed wavelength, propagation distance z and high turbulence level

In Figure 2.5, for different radial and angular mode numbers, the radius of curvature of the Laguerre-Gaussian beam variations are plotted vs. source size at fixed wavelength, propagation distance z and high turbulence level ($C_n^2 = 10^{-14} \text{ m}^{-2/3}$). Figure 2.5 shows that high turbulence levels diminish the radius of curvature as expected.

From Figures 2.4 and 2.5, it is possible to say that high turbulence decreases the radius of curvature of the Laguerre-Gaussian beam. As in Figures 2.1, 2.2 and 2.3, the Laguerre-Gaussian beam follows the trend of a Gaussian beam.

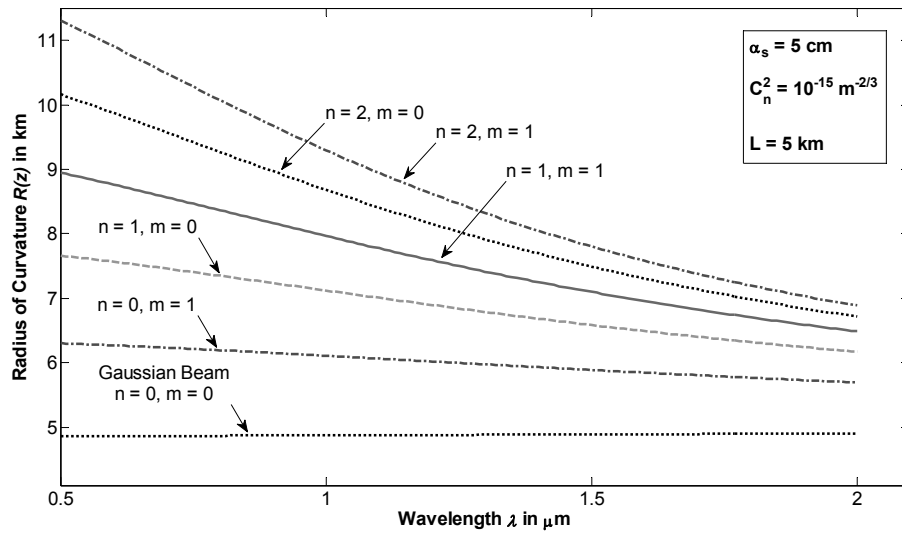


Figure 2.6 Radii of curvatures vs. wavelength at fixed source size, propagation distance z , and moderate turbulence level

In Figure 2.6, for different radial and angular mode numbers, the radius of curvature of the Laguerre-Gaussian beam variations are plotted vs. wavelength at fixed source size, propagation distance z , and moderate turbulence level ($C_n^2 = 10^{-15} \text{ m}^{-2/3}$). Figure 2.6 shows that the radii of curvatures decrease with increasing wavelength for all orders of the Laguerre-Gaussian beam except for the Gaussian beam ($n = 0, m = 0$). The Gaussian beam slightly increases with increasing wavelength.

CONCLUSION

In this study, analytical formulation for the radius of curvature has been developed for the Laguerre-Gaussian beam in turbulent atmosphere. When related terms with “associated Laguerre polynomials” are eliminated, this formula shows that the radius of curvature of the Laguerre-Gaussian beam is reduced to the radius of curvature of a pure Gaussian beam. In this point, accuracy of equation (2.23) is shown by taking $n = 0$, $m = 0$ and $C_n^2 = 0$. That is, equation (2.23) will be reduced to equation (1.26). This formula is analyzed numerically by using Matlab under certain conditions. All figures show that the radius of curvature of the Laguerre-Gaussian beam acts in accordance with radius of curvature of Gaussian beam ($n = 0, m = 0$) at all radial and angular mode numbers. Also, it is observed that increasing turbulence levels causes a decrease in radii of curvatures of Laguerre-Gaussian and Gaussian beams ($n = 0, m = 0$). That is, increasing turbulence causes the wavefront to bend as expected. Meanwhile increasing turbulence reduces the difference between radii of curvatures of Laguerre-Gaussian beams, having different radial and angular mode numbers.

From Table 2.1, for all radial and angular mode numbers, it is seen that Laguerre-Gaussian beam has longer Rayleigh range than those for the Gaussian beam at moderate and high turbulence levels. In the free space, because of Laguerre-Gaussian beam acts as a Gaussian beam, all the beams have same Rayleigh range.

For different source sizes at a fixed propagation distance, the radius of curvature of the Laguerre-Gaussian beam follows the trends for the Gaussian beam at different turbulence levels. Radii of curvatures of the Laguerre-Gaussian and the Gaussian beams are around the propagation distance for smaller source sizes. With larger source sizes, radii of curvatures of these beams will increase. Also, the radius of curvature of the Laguerre-Gaussian beam decreases with increasing wavelength except lowest radial and angular mode numbers (Gaussian beam).

Based on this information, beam type can be selected properly for the optical link's requirements.

REFERENCES

- [1] Özsoy, S. (2006), Fiber Optik (2nd.Ed), Birsen Yayımevi, İstanbul, TR.
- [2] Andrews, L.C., Philips, R.L. (2005), Laser Beam Propagation through Random Media (2nd Ed.), Spie Press, Bellingham, Washington USA.
- [3] Heinz Willebrand, Ph.D., and Baksheesh S. Ghuman (2001), Free Space Optics: Enabling Optical Connectivity in Today's Networks, (1st Ed.), SAMS, Indiana USA.
- [4] Eyyuboğlu, H.T., Ji, X. (2010) An Analysis on Radius of Curvature Aspects of Hyperbolic and Sinusoidal Gaussian Beams, Springer-Verlag, 1-2. Vol. 101.
- [5] Eyyuboğlu, H.T., Baykal, Y.K., Ji, X.L. (2010) Radius of Curvature Variations for Annular, Dark Hollow and Flat Topped Beam in Turbulence, Springer-Verlag, 4. Vol. 99.
- [6] Eyyuboğlu, H.T., Baykal, Y., Ji, X. (2010) Scintillations of Laguerre Gaussian beams, Springer-Verlag, 4. Vol. 98.
- [7] Eyyuboğlu, H.T., Baykal, Y., Sermutlu, E., Cai, Y. (2008) Scintillation Advantages of Lowest Order Bessel–Gaussian Beams, Springer-Verlag, 2. Vol. 92.
- [8] K.F. Riley, M.P. Hobson and S. J. Bence (2006), Mathematical Methods for Physics and Engineering, (3th Ed.), Cambridge University Press.
- [9] Saleh, B.E.A., Teich, M.C. (2007), Fundamentals of Photonics (2nd Ed.), Wiley.
- [10] Gradshteyn, I.S., Ryzhik, I.M. (2007), Table of Integrals, Series, and Products (7th Ed.), Elsevier.
- [11] Weisstein, Eric W. “Associated Laguerre Polynomial.” from MathWorld A Wolfram Web Resource:
<http://mathworld.wolfram.com/AssociatedLaguerrePolynomial.html>

- [12] Rowe, G. “Laguerre Polynomials – Normalization” from Physicspages
Web Resource:
<http://physicspages.com/2011/06/14/laguerre-polynomials-normalization>
- [13] Siegman, Anthony E. (1986), Lasers, University Science Books, Mill Valley, CA.

CURRICULUM VITAE

PERSONAL INFORMATION

Surname, Name: Çay, Saim

Nationality: Turkish (TC)

Date and Place of Birth: 22 May 1983, ADANA/Saimbeyli

Marital Status: Single

Phone: 0505 238 23 19

email: saimcay@gmail.com

EDUCATION

Degree	Institution	Year of Graduation
BS	Çanakkale 18 Mart Univ. <u>Physics</u>	2007
High School	Söke High School	2002

WORK EXPERIENCE

Year	Place	Enrollment
2008	<u>Türksat</u>	Intern

FOREIGN LANGUAGES

Advanced English

HOBBIES

Computer programming, travel, music, playing guitar, cinema, reading book